Thermal Simulation of a Pyrotechnic Solid-Propellant Gas Generator

Mohammad K. Alkam[a,*], P. Barry Butler[b]

[a]*Department of Mechanical Engineering Jordan University of Science and Technology Irbid, Jordan*

[b]*Department of Mechanical and Industrial Engineering, The University of Iowa, Iowa City, IA 52242,U.S.A*

Abstract

The current work presents a numerical simulation of the thermal operation of a pyrotechnic solid propellant gas generator undergoing a tank test. The effect of several parameters on the thermal characteristics of the system under consideration is investigated. These parameters include heat loss to the ambient, heat transfer to the hardware elements of the present system, and ambient temperature. The question of the applicability of tank test results to auto airbag systems has been addressed. In the present work, it has been concluded that the thermal performance of present system is significantly sensitive to heat transfer to the tank wall and to the value of the ambient temperature.

Keywords: Pyrotechnic; Gas Generator; Airbag; Tank-Test.

Nomenclature

Variable	Definition	Dimension
A	area	cm^2
a	propellant burning rate prefactor	$cm/(s\text{-}MPa^n)$
C_d	discharge coefficient	
C_p	constant pressure specific heat	J/g-K
C_v	constant volume specific heat	J/g-K
d	grain diameter	cm
H	enthalpy	J/g
H_f	enthalpy of formation	J/g
j	computational cell index	
k	species index	
kk	total number of species	
L	length	cm
m	mass	g
$\dot{m}$	mass production rate	g/s
N	number of propellant grains	
P	pressure	N/m^2
Q	energy transfer	J
$\dot{Q}$	energy transfer rate	J/s
r	burn depth	cm
R	gas constant = R_u/W	J/g-K
RI	inner radius	cm
RO	outer radius	cm
R_u	universal gas constant	J/mol-K
T	temperature	K
To	ambient temperature	K
ΔT	change in temperature (T-298 K)	K
U	internal energy	J/g
V	volume	cm^3
W_k	molecular weight of species k	g/mol
W	mixture molecular weight	g/mol
Y	mass fraction	

Greek

γ	specific heat ratio	
ρ	density	g/cm^3
$\dot{\omega}$	gas-phase mass production	g/s
ϕ	volume fraction of condensed-phase species	
σ	propellant temperature-sensitivity coefficient	K^{-1}

Subscripts

c	combustion chamber
eff	effective
gen	generant (propellant)
gr	grain
ign	ignitor
j	gas cell index
k	species index
M	hardware cell index
P	product
p	plenum
ref	reference state (298 K, 1 atmosphere)
R	reactant
t	discharge tank

Superscripts

H	hardware
n	propellant burning-rate pressure index
gas	gas-phase

* Corresponding author. alkam@just.edu.jo.

cond   condensed-phase
o   standard-state

1. Introduction

Solid propellant gas-generators have several engineering applications. Among these applications are pilot emergency escape systems, missile launching, powering actuators and valves, and short-term power supplying [1]. Of special interest to the present work is the performance of solid propellant gas generators used in automotive applications. Current automotive applications include inflation devices for driver, passenger and side impact airbags and knee bolsters, and piston actuators for automatic seat belt tensioners. Contemporary airbag systems can be classified into two major groups based on the configuration used to produce gas for inflating a vehicle airbag [2]. The first group is referred to as "pyrotechnic" in which the air bag is inflated solely by rapid gas production from a solid propellant. The second group is referred to as "augmented" in which hot gases produced from a solid propellant are diluted by an ambient-temperature, high-pressure stored gas before the gas mixture is discharged into the airbag. However, earlier airbag configurations (over the 1960's) relied solely on pressurized, ambient-temperature stored gas to inflate airbags [3].

There are several issues of considerable concern to the designer of an automotive airbag system. These issues include: 1) the size of the inflator, 2) the volume ought to be occupied by the inflated airbag, 3) the transients of the airbag operation, especially the time duration of the inflating process, 4) the force exerted by the airbag on the driver and/or the passenger upon the inflating process, 5) the sensitivity of the airbag-system performance to a wide range of ambient conditions, 6) the reliability of the airbag system over a relatively long period of time that spans over 20 years, and 7) the thermophysical properties of the utilized propellant. In an investigation conducted by Berger and Butler [4], the authors studied the decomposition behavior of three condensed-phase propellants commonly used in airbag industry. These propellants are 1) sodium-azide (NaN_3), 2) a non-azide propellant containing azodicarbinamide (ADCA), and 3) a double-based propellant (DB). In their work, Berger and Butler studied several thermophysical properties of the above mentioned propellants including a) the flame temperature and chemical composition of the product gases, b) the number of gaseous moles produced per mass of condensed phase propellant consumed, c) the condensed-phase (slag) production of each propellant, and d) and the toxicity of gas-phase combustion products. It has been concluded that there is a trade off between the advantage of producing large number of gaseous moles per unit mass of solid propellant and the advantage of having a lower flame temperature. The study showed that among the three propellants under consideration, NaN_3 has the lowest flame temperature, but also the lowest gas production per unit mass of propellant. The study concluded also that there is a negative correlation between the flame temperature and the amount of slag produced. In another study, Ulas et al. [5] conducted an experimental investigation on the determination of ballistic properties

and burning behavior of a composite solid propellant for airbag application. In their article, it was reported that the pressure exponent was found to be a strong function of the initial propellant temperature. They also introduced the values of the activation energy and the pre-exponential factor of the Arrhenius equation.

There appears to be a current demand for novel designs of airbag systems such that the output of the airbag operation could be controlled according to different crash conditions. These types of airbags are referred to as "smart" airbags. One method being studied for controllable output is to add a second solid-propellant combustion chamber to a standard augmented gas generator [6]. The traditional single-combustor gas generator is designed around a single operating state. For example, in the U.S. this is specified as being sufficient to protect an unbelted, 74.5-kg adult in a 48-km/hr frontal collision. All other operating conditions are considered off-design. The augmented, dual-combustion chamber design presented in ref. [6] can be optimized for three operating conditions to, consequently, have a more uniform off-design performance. The wider range of acceptable operation is a result of dynamic controllability of the discharge process to match the kinematics of the occupant as they are thrown towards the deploying airbag.

In airbag industry, the performance of an airbag inflator is often evaluated by conducting what is commonly called "tank test". In a tank test, the combustion products are allowed to flow into a rigid tank that is initially filled with ambient air; in the meanwhile pressure and temperature histories of the combustion products in the tank are observed. Besides, the final product composition is measured. In an auto airbag operation, the combustion products flow into an inflatable airbag rather than a rigid tank. From a thermal point of view, that is the major difference between the operation of an auto airbag and a tank test operation, given that all other design and operating conditions are similar. The question remains whether the tank test provides satisfactory description of the auto airbag inflating process. One important issue is the amount of energy lost within the hardware components of the system under consideration, especially the tank wall. This energy plays a major role in the thermal behavior of the products of combustion. Hence, investigating the amount of energy lost within each hardware component could help judge whether the tank test is an acceptable representation of the auto airbag operation. Besides, it would provide a better understanding of the thermal transients of the airbag operation. In a recent study, Sinz and Hermann [7] have developed an algorithm for simulation of an airbag deployment.

In the present work, it is intended to evaluate the performance of a pyrotechnic solid-propellant gas generator in a conventional tank-test environment. Special emphasis is put on the heat balance characteristics of the system at hand. The analysis is performed using AIM; a program designed to simulate the transient, thermochemical events associated with the firing of a solid propellant gas generator [8]. AIM models the processes of gas generation and discharge which are highly nonlinear events governed by first principles (i.e., solving complete conservation equations, variable specific heats, mixture mixing rules, etc.). AIM also includes the dynamics of
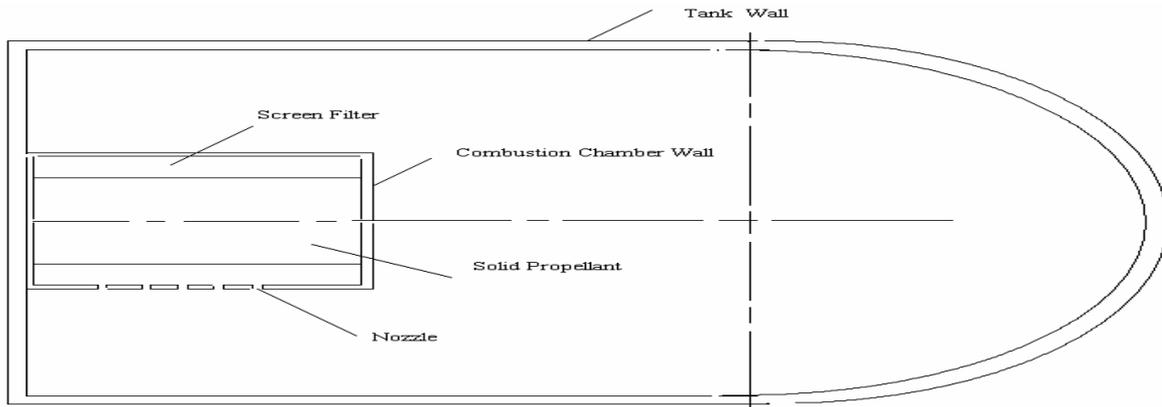
Figure 1: Schematic Diagram of the present problem/

coupled events such as ignition, heterogeneous combustion, particle filtering, heat transfer, phase change, and mass discharge. Further demands arise when the simulation also takes into consideration the temperature gradients within the walls of the hardware components.

2. Poblem Description

The present work introduces thermal analysis of a conventional pyrotechnic solid propellant gas generator. This gas generator is based on the approximate design specifications of an inflator of a passenger-side airbag. The inflator at hand delivers the combustion products into a constant volume tank such that the pressure inside the tank is elevated into a certain value without exceeding a maximum tank pressurization rate. A schematic diagram of the setup under consideration is shown in Fig. 1. The combustion chamber contains the main propellant along with a small amount of ignitor propellant. The mass of propellant occupies a portion of the total volume within the combustion chamber. Also, within the combustion chamber is a metallic screen used to capture condensed-phase particulate and to cool the exiting gases. The screen, with a specified mass, has a hollow cylindrical shape and it is located at the inner wall of the combustion chamber. The combustion products exit the combustion chamber through an array of nozzles each of individual flow characteristics. The nozzles are initially covered with a burst foil that seals the interior of the combustion chamber from the surrounding tank. The burst foil is designed to rupture when the pressure within the combustion chamber reaches a predetermined burst pressure. The discharge tank is a constant-volume cylindrical vessel with a hemispherical top. It has a volume that is several orders of magnitude larger than the volume of the gas generator and it has no exit nozzles. The only inlet into the discharge tank comes from the exit nozzles of the combustion chamber. Initially, the discharge tank contains air at atmospheric conditions.

3. Mathematical Model

The propellant used throughout this study is sodium-azide ($NaN3$). It is assumed that the combustion process proceeds at an equilibrium state during the complete burning process of the propellant. It is also assumed that the surrounding conditions do not deviate substantially during the combustion process. Therefore, the distribution of product species calculated at one flame state are assumed to be the same throughout the combustion process [9]. With these assumptions an adiabatic flame temperature calculation can be performed at an estimated average pressure within the combustion chamber.

The standard JANNAF [10] species database was used for calculating the thermochemical properties of the products of combustion for the propellant. Product species were chosen from this database by minimizing the Gibb's free energy of the reacting system within a specified tolerance while satisfying the elemental population constraint. PEP [11], a thermochemical equilibrium calculation program, was used to solve the system of equations to determine the adiabatic flame temperature and the relative amounts of product species.

The following premises dictate the mathematical formulation of the present model:
1. Gas-phase and condensed-phase combustion products are composed of multiple species.
2. Specific heats of the species present are temperature-dependent.
3. The existence of extreme turbulent mixing upon gas deployment results in much shorter fluid mixing time scales than diffusion time scales. This motivates the assumption of well-mixed gases, and hence gaseous and condensed-phase products are assumed spatially uniform within the combustion chamber, on the one hand, and the tank, on the other.
4. The use of the filtering screen restricts the solid propellant combustion to the combustion chamber.
5. Ignition of the solid propellant is represented by an empirical expression that was determined from experimental data.
6. Heat transfer within the combustion chamber and the tank walls is axisymmetric, i.e. the temperature within the hardware walls is function of axial and radial coordinates in addition to time.

The present conservation equations are derived by applying conservation principles of mass and energy to the computational domain under consideration. The computational domain of interest is divided into 1) three gas computational cells corresponding to the combustion chamber, the tank, and the ambient, respectively, and 2) a prescribed number of hardware cells that represent the combustion chamber and the tank walls. These cells are obtained by dividing the hardware walls into a number of finite element cells. The distribution of the gas
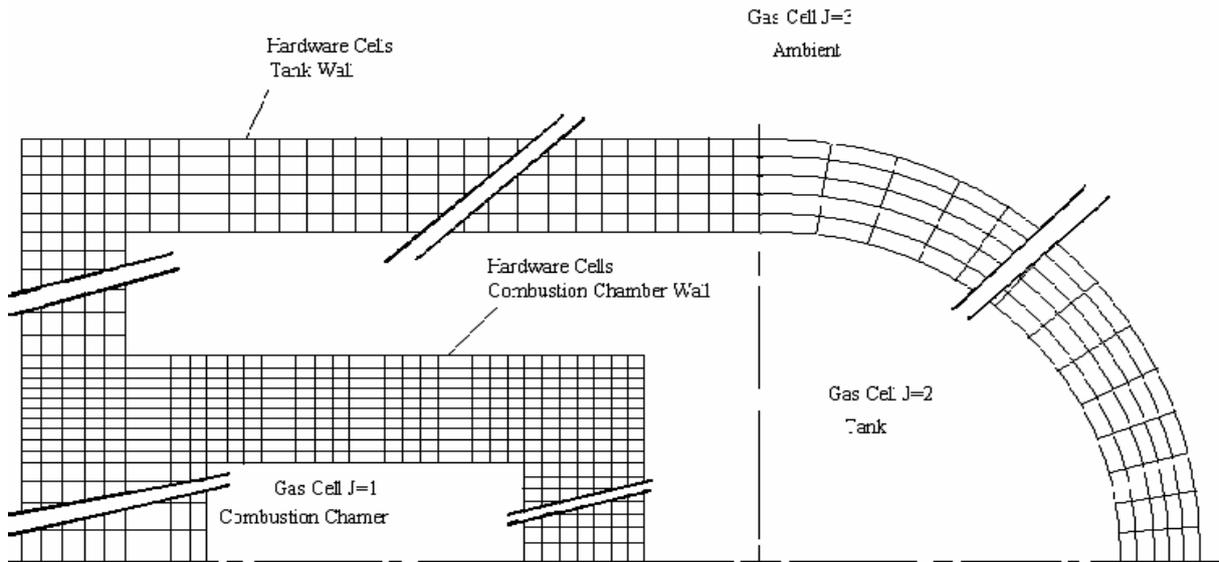
Figure 2. Distribution of the hardware Computational cells of the combustion chamber and the tank walls

computational cells as well as the hardware cells is depicted in Fig. 2.

Taking into consideration the set of assumptions listed above, the conservation equations of species mass and energy are applied to the individual volumetric cells within a gas generator system. The gas cells shown in Fig. 2 are designated with the index j, whereas the j=1 for the combustion chamber, j=2 for the tank, and j=3 for the ambient. The gas within the volumetric cell j of size V_j, is well mixed (spatially uniform) and has properties P_j, T_j, ρ_j. The mass inflow from cell j-1 is uniform across the inlet area and has properties P_{j-1}, T_{j-1}, and H_{j-1} where H_{j-1} is the enthalpy of the mixture in cell j-1. The hardware cells shown in Figs. 2 are designated with the index M, where M varies from 1 to Mt. Each hardware cell has a volume V_M, and has a temperature T_M.

For each gas-cell control volume j depicted in Figure 2, the conservation of species equation takes the following form:

$$\frac{dm_{k,j}}{dt} = Y_{k,j-1}\dot{m}_{j-1} - Y_{k,j}\dot{m}_j + \dot{\omega}_{k,j} + \dot{m}_{gen,k,j} \quad (1)$$

The sum of $\dot{\omega}_{k,j}$, the gas-phase mass production rate, and $\dot{m}_{gen,k,j}$, the mass addition due to propellant decomposition, represent the rate of mass production within the control volume, and Y_k is the mass fraction for species k. The energy equation for each gas cell is written as Formula 2 :

$$\frac{dT_j^{gas}}{dt} = \frac{1}{m_j^{gas} C_{vj}^{gas}} \left[\begin{array}{l} \sum\limits_{k=1}^{kk} (U_{k,j}\dot{\omega}_{k,j}) + H_{j-1}^{gas}\dot{m}_{j-1}^{gas} - H_j^{gas}\dot{m}_j^{gas} \\ + \dot{Q}_j^{gas} + H_j^{gas}\dot{m}_{genj}^{gas} + P_j V_j^{gas} \dfrac{d\phi_j}{dt} \end{array} \right]$$

The production of gas from a burning propellant is dependent on the propellant surface regression rate $\dot{r}_{gr}$, instantaneous propellant grain surface area A_{gr}, and propellant density ρ_{prop}. The propellant burning rate is modeled as a function of pressure and variation from

ambient temperature ΔT and is represented by the form [12].

$$\dot{r}_{gr} = a e^{\sigma \Delta T} P^n \quad (3)$$

Here, r_{gr} is the burn depth measured from the initial surface of the propellant. Equation 3 is a typical burn-rate function for propellants under quasi-steady-state pressure conditions. The variation of the propellant grain surface area, on which a flame is propagating, with burn depth, is primarily dependent on the geometry of the propellant grain as well as flame spreading characteristics and can also change due to grain fracture. The variation of the propellant grain surface area, on which a flame is propagating, with burn depth, is called the form function of the grain and is primarily dependent on the geometry of the propellant grain as well as flame spreading characteristics and can also change due to grain fracture. For this study, it is assumed that the form function is only a function of grain geometry. Thus, it is assumed that flame spread is instantaneous on the grain surface at the time of ignition and no grain fracture occurs. Analyzing the regression of the propellant grain shape can develop a form function based solely on geometry. For all results presented herein, the propellant grains are modeled as solid right circular cylinders, initially 1.1 cm in length and 4.1 cm in diameter which burn uniformly on all exposed surfaces. The right circular cylinder geometric shape provides a well-defined mathematical relationship between surface area of the propellant grain and the burn depth.

The total rate of mass addition to the system due to propellant decomposition is:

$$\dot{m}_{prop} = N_{gr} A_{gr}\ \rho_{prop}\ \dot{r}_{gr} \quad (4)$$

Combining the rates of mass production rate from the propellant and ignitor charge according to Eq. (5) provides closure for the addition of mass to the system and completes the necessary relations to conserve mass within the gas generator system.

$$\dot{m}_{gen} = \dot{m}_{ign} + \dot{m}_{prop} \qquad (5)$$

The mass flow exiting each volumetric cell through the local nozzles is classified as either in the sonic or subsonic flow regime, depending on the pressure difference between the adjacent cells and the specific heat ratio of the gaseous mixture within the volumetric cell from which the gases are exiting. The choked flow critical condition is calculated to determine whether a sonic or subsonic flow condition exists for the mass flow between two cells using the above parameters. Applying the fundamental laws of gas dynamics, the gas-phase mass flow rate is determined from the following sonic and subsonic relations.

Subsonic formula 6:

$$\dot{m}^{gas} = A_{flow} C_d \sqrt{\frac{2\gamma}{\gamma-1} P_+ \rho_+ \left(\left(\frac{P_+}{P_-}\right)^{\frac{2}{\gamma}} - \left(\frac{P_+}{P_-}\right)^{\frac{\gamma+1}{\gamma}} \right)}$$

Sonic formula 7:

$$\dot{m}^{gas} = A_{flow} C_d \sqrt{\gamma P_+ \rho_+} \left(\frac{2}{\gamma+1}\right)^{\frac{\gamma+1}{2(\gamma-1)}}$$

In Eqs. (6) and (7), A_{flow} and C_d are the respective flow area and discharge coefficient for the given nozzle [13]. The subscripts '+' refers to the high-pressure chamber and '-' refers to the low-pressure chamber.

The term (Q_j^{gas}) that appears in Eq. (2) represents the net heat transfer between the gas in cell J and all the hardware cells that are in direct thermal communication with the gas in this specific cell. The calculation of this term is based on an effective heat transfer coefficient, h_{eff}, obtained from Nusselt number correlations according to the geometrical and flow conditions of the local flow [8].

The energy equation for each hardware cell is written as:

$$\frac{dT_M^H}{dt} = \frac{\dot{Q}_M^H}{m_M^H C_{vM}^H} \qquad (8)$$

where the term $(\dot{Q}_M^H)$ represents the net heat transfer exchange between the hardware cell M and all the computational cells that are in direct thermal communication with the hardware cell M. This term includes: 1) heat exchange between a specific hardware cell and the adjacent gas cell $(\dot{Q}_M^H)$, and 2) heat exchange between a specific hardware cell and all other adjacent hardware cells. This part of heat exchange is calculated in a quasi equilibrium fashion assuming the hardware material has constant physical properties. In other words, the heat flux between two adjacent hardware cells in certain direction equals the thermal conductivity multiplied by the temperature gradient between the two cells in that direction divided by the appropriate length scale.

Individual gas- and condensed-phase chemical species are tracked throughout the numerical simulation, thus requiring thermodynamic properties for each chemical species over a wide range of conditions. A fourth-order polynomial expansion in temperature is used to represent the standard-state, constant-pressure specific heat data for the individual species $C_{p,k}^o(T)$. Standard-state enthalpy of the species can be determined by the fundamental thermodynamic relationship:

$$H_k^o(T) = \int_{T_{ref}}^{T} C_{p,k}^o(T) + H_{f,k}^o(T_{ref}) \qquad (9)$$

All condensed-phase species are considered incompressible:

$$\rho_{cond,j} = \text{constant} \qquad (10)$$

where R_j, the gas constant for cell j, is dependent on the local mixture molecular weight: $W_j = \Sigma X_k W_k$
From this derivation, a system of ordinary differential equations is developed to express the time derivatives of all dependent variables: gas- and condensed-phase temperatures, individual species mass, and gas pressure within each gas cell, in addition to hardware temperatures. These differential equations combine with the constitutive relations to form the governing equations for the gas generator systems.

4. Discussion of Results

The results of the present work are obtained using a stoichiometric mixture of NaN_3 and Cu_2O. This composition is often used in airbag industry. A thermochemical equilibrium code [11] has been used to characterize the equilibrium composition of the present propellant. Table 1 describes the composition of both the reactants and the products of combustion of the problem under consideration, given that the reactants exist at ambient conditions and the products exist at the adiabatic flame temperature of the present mixture. Table 1 shows that 60.412 % of the product mass is in condensed phase, while the gaseous products are mainly composed of N_2. Hence, the gas-phase reactions within the combustion products are neglected and all chemical species present at the calculated adiabatic flame temperature are assumed to be chemically frozen.

The present results are obtained using the software AIM [8]. AIM incorporates the chemical kinetic package CHEMKIN [14] to evaluate thermodynamic properties for all species present. It also uses the ordinary differential equations solver LSODE [15] to solve the resulting set of ordinary differential equations along with the proper initial conditions numerically. Besides, all chemical species are characterized in terms of standard-state, temperature-dependent specific heat functions, heats of formation and entropies of formation. These chemical species data are taken from JANAF thermodynamic tables [10]. Table 2 shows the initial, operating, and design conditions that

have been used throughout the present computations. These conditions resemble a generic inflator system.

The operating and design conditions that appear in Tables 1 and 2 have been used to produce the results of present case study. Throughout this text, these conditions will be referred to as "basic conditions". All the figures in the present work have been produced using the basic conditions unless otherwise stated. AIM computations have been verified in ref. [6]. The authors presented a comparison between AIM computations and analytical solutions for two standard problems, namely, isentropic and isothermal dishrags of constant volume pressurized chamber.
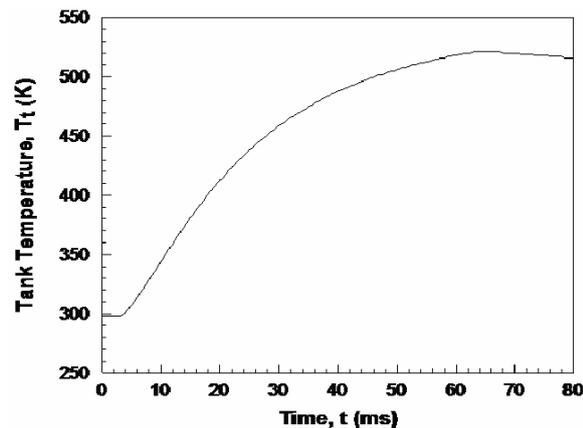
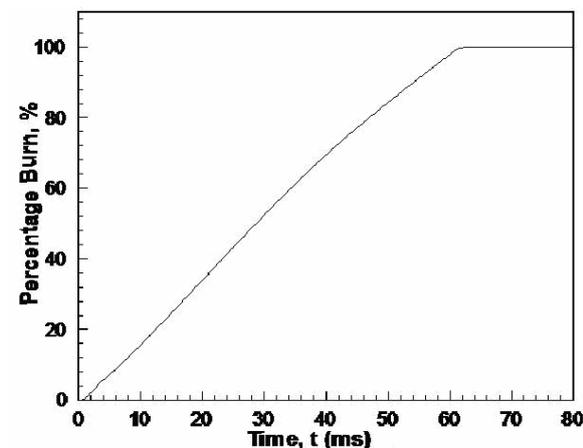Figure 3. Temperature history inside the tank.

Figure 4. History of the fuel precentage burn.

The temperature history of the gases inside the tank is shown in Fig. 3. The maximum value of the gas-temperature inside the tank is reached after about 60 ms from the beginning of combustion. At this instant, almost all of the solid propellant have just been burned as shown in Fig. 4.

The performance of an airbag inflator is commonly evaluated by several parameters. Among these parameters are the maximum pressure rise-rate, the peak pressure and temperature within a standard discharge tank, and the time integral of the pressure inside the discharge tank (pressure impulse). The maximum pressure rise-rate affects the airbag transients upon the inflating process. The peak pressure and temperature, and the pressure impulse inside the tank are key issues in the safety considerations of a vehicle occupant. The pressure impulse provides a

Table 1. Chemical composition of solid propellant and combustion products.

Propellant Formulation				
Component	Phase	Mass %	Mole %	Molecular Weight
NaN_3	S	60.998	77.488	65.01
Cu_2O	S	39.002	22.512	143.08
Combustion Products				
N_2	G	39.451	53.807	28.01
Cu	S	34.661	20.842	63.54
Na	L	8.846	14.702	22.99
Na	G	0.136	0.227	22.99
Na_2O	S	16.905	10.421	61.98

Table 2. Present system parameters.

Variable (units)	Value
Combustion chamber material	Aluminum
Nozzles (Diameter(m) , Number)	(0.006,18) (0.005,12)
$\rho_C (kg/m^3)$	2770
$\rho_t (kg/m^3)$	7854
Filter material	Carbon Steel
$m_C (kg)$	0.68
$m_{Filter} (kg)$	0.5467
$L_C (m)$	0.2712
$L_{Filter} (m)$	0.247
$m_P (kg)$	0.445
N	14
$RI_C (m)$	0.02615
$RI_{Filter} (m)$	0.0205
$RO_C (m)$	0.03055
$RO_{Filter} (m)$	0.0255
Tank material	Carbon Steel
$V_C (m^3)$	0.0005826
$V_t (m^3)$	0.06

computations with and without heat transfer to the tank walls.

measure of the momentum transferred to a vehicle occupant. The peak pressure within the discharge tank provides a measure of the discharged energy of an inflator system. In airbag industry, the conventional tank test has been used to evaluate the performance of airbag inflators. The question that rises is whether or not the tank test conditions resemble the actual operation of the airbag. There is a considerable difference between heat transfer to the wall of the discharge tank and heat transfer to the airbag. This may lead to a significant difference between the thermal behavior of an airbag operation and that of a tank test. It is intended to investigate the sensitivity of the tank test output to the amount of heat transfer to the tank wall. This could help evaluate the need for more research on the airbag itself rather than the tank test. For that purpose, the pressure history inside the tank is plotted in Fig.5. The figure compares the present calculations of the pressure transients with a similar case but without heat transfer to the tank wall. It is clear that both the peak pressure and the pressure rise-rate are considerably sensitive to heat transfer to the tank wall. This result

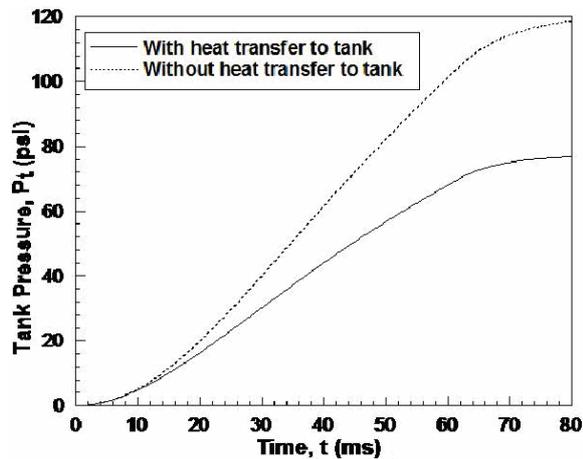suggests that one should be careful upon applying the tank test results on airbag systems directly.

Figure 5. Computation of the tank pressure history. Comparison between

The high sensitivity of the thermal characteristics of the present system to heat transfer (observed in Fig. 5) creates an interest in the heat transfer issue of airbag systems. It is interesting to perform an energy balance to find out how much energy is lost through heat transfer to the hardware during the operation of the current system. Figure 6 presents the history of the integrated amount of heat transfer to the combustion chamber wall, the screen filter, the tank wall, and the ambient. It Fig. 6, it is shown that the heat loss to the ambient is negligible. At the same time, the tank wall absorbs energy the least, while the combustion chamber wall absorbs energy the most among the hardware elements. However, Fig. 5 shows that the present system is significantly sensitive to the heat transfer to the tank wall. Figures 5 and 6 demonstrate the importance of heat transfer to the hardware in modeling airbag systems.
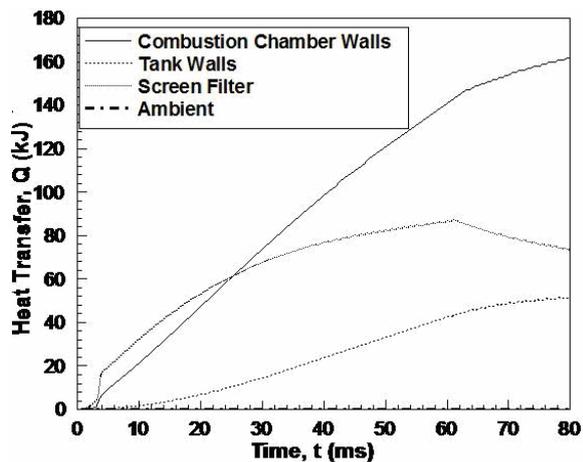

Figure 6. History of the heat absorbed by the combustion chamber walls, the tank walls, the screen filter, and the ambient.

An important issue in the design of airbags systems is the sensitivity of the airbag performance to ambient conditions. Airbags operate under a wide range of ambient temperatures that might span from 230 to 320 K. It is essential to investigate the performance of the present sample case under a broad extent of ambient temperatures. The effect of ambient temperature on the tank pressure
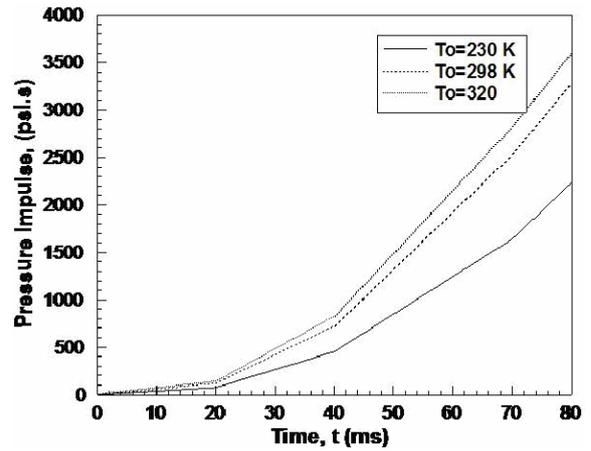

Figure 7. Effect of ambient temperature on the history of the pressure impulse.
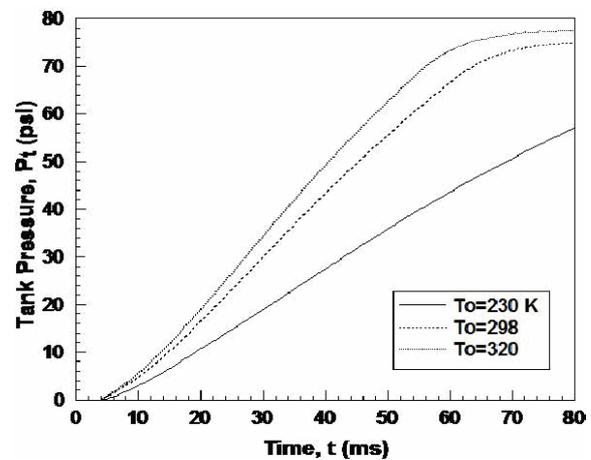

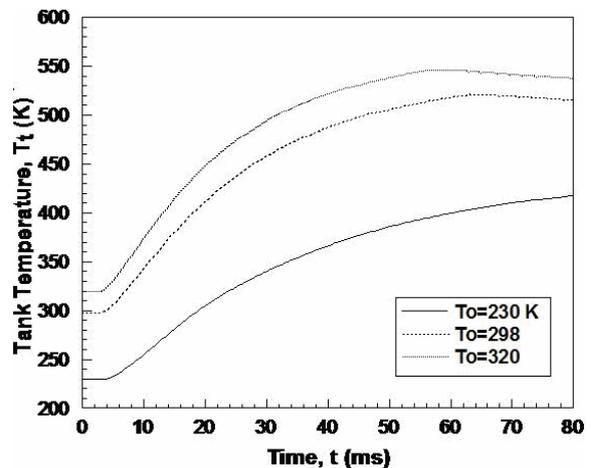Figure 8. Effect of ambient temperature on tank pressure history.

Figure 9. Effect of ambient temperature on tank temperature .

impulse is shown in Fig. 7. The figure shows that the tank pressure impulse at an ambient temperature of 320 K is around 50 % larger than that at an ambient temperature of 230 K. Further explanation of the effect of ambient temperature of the thermal characteristics of the present system is presented in Figs. 8, 9, and 10. Figure 8 shows that as the ambient temperature increases the maximum pressure inside the tank as well as the maximum pressure rise-rate increases considerably. The increase in ambient temperature increases the temperature level of the inflating
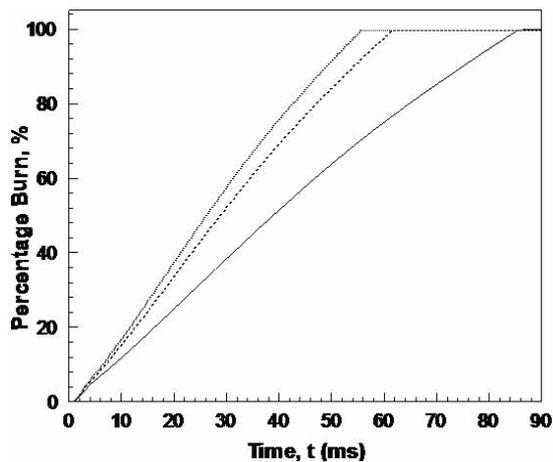
Figure 10. Effect of ambient temperature on history of fuel precentage burn.

process, and eventually increases the maximum temperature inside the tank as shown in Fig. 9. This explains the increase in the maximum tank pressure due to higher ambient temperature. The marked effect of the ambient temperature on the burn rate that is shown in Fig. 10 explains the effect of ambient temperature on the maximum pressure rise-rate. The figure shows that the present solid propellant burns faster at higher ambient conditions. Consequently, the mass flow rate of the product-gases into the tank increases and results in a faster rise in the tank pressure.

5. Conclusions

In the present work, a pyrotechnic solid propellant gas generator has been analyzed. The current results presented are intended to show the thermal characteristics of a generic design of an airbag inflator in a tank test. For the current operating and design conditions, the following conclusion are drawn:

1. The heat loss to the ambient is negligible.
2. The tank pressure history is sensitive to heat transfer to the tank wall. This makes it necessary to incorporate accurate heat transfer modeling for heat transfer to the hardware elements of airbag system.
3. The tank test results should not be applied directly to auto-airbags because the significant difference in heat transfer between the hot gases and the tank wall on the one hand, and the hot gases and the airbag, on the other, affect the tank pressure history.
4. It has been concluded that the thermal performance of the system under consideration can be significantly affected by the ambient temperature. If the ambient temperature rises from 230 to 320 K, the tank pressure

impulse increases by 50 %, the combustion time decreases by 35 %, the maximum tank pressure increases by 20 %, and the maximum tank temperature increases by 27 %.

References

[1] Sutton G P. Rocket propulsion elements. 6th Edition. John Wiley and Sons; 1992.
[2] P.B. Butler, J. Kang, H. Krier, "Modeling and numerical simulation of the internal thermochemistry of an automotive airbag inflator". Progress in Energy and Combustion Science, Vol. 19, 1993, 365-382.
[3] T.H. Vos, G.W. Goetz, "Inflatable restraint systems: Helping save lives on the road". TRW Space and Defense Quest, Winter Issue, 1989.
[4] J.M. Berger, P.B. Butler, "Equilibrium analysis of three classes of automotive airbag inflator propellants". Combustion Science and Technology, Vol. 104, No. 1-3, 1995, 93-114.
[5] A. Ulas, G.A. Risha, K.K Kuo, "Ballistic properties and burning behavior of an ammonium Perchlorate/Guanidine Nitrate/Sodium Nitrate airbag solid propellant". Fuel, Vol. 85, 2006, 1979–1986.
[6] J.J. Freesmeier, P.B. Butler, P. Barry, "Analysis of a hybrid dual-combustion- chamber solid-propellant gas generator". Journal of Propulsion and Power, Vol. 15, No. 2, March-April, 1999.
[7] W. Sinz, S. Hermann, "The development of a 3D-navier–stokes code for the simulation of an airbag inflation". Simulation Modeling Practice and Theory, Vol. 16, 2008, 885-899.
[8] Butler P B, Krier H. Airbag Inflator Model User's Guide. Champaign: Combustion Sciences Inc.; 1997.
[9] R.G. Schmitt, P.B. Butler, J.J. Freesmeier, "Performance and CO Production of a Non-Azide airbag propellant in a pre-pressurized gas generator". Combustion Science and Technology, Vol. 122, 1997, p. 306.
[10] Chase M W, Davies C A, Downey J R, Frurip D J, McDonald R A, Syverud A N. JANAF thermochemical tables. 3rd Edition. American Chemical Society; 1985.
[11] Cruise D R. Theoretical computations of equilibrium compositions, thermodynamic properties, and performance characteristics of propellant systems, PEP equilibrium code. NWC Technical Report, NWC TP 6037; 1973.
[12] K.K. Kuo, M. Summerfield, "Fundamentals of solid-propellant combustion (Progress in Astronautics and Aeronautics)". AIAA, Vol. 90, 1984, 622-623.
[13] Zucrow M J, Hoffman J D. Gas Dynamics. Vol. 1. John Wiley and Sons; 1976.
[14] Kee R J, Miller J A, Jefferson T H. CHEMKIN: A general-purpose, problem-independent, transportable, FORTRAN chemical kinetics code package. Sandia National Laboratories, *SAND 80-8003,* Livermore, CA; 1980.
[15] Hindmarsh A C. *LSODE* Software. Lawrence Livermore National Laboratories, Livermore, CA; 1980.